0026-895X/96/061021-12$3.00/0

MOLECULAR PHARMACOLOGY, 49:1021–1032 (1996).



# Antagonist Conformations within the $\beta_2$-Adrenergic Receptor Ligand Binding Pocket

GREGORY H. HOCKERMAN,[1] MARK E. GIRVIN, CRAIG C. MALBON, and ARNOLD E. RUOHO

*Departments of Pharmacology (G.H.H., A.E.R.) and Biomolecular Chemistry (M.E.G.), University of Wisconsin School of Medicine, Madison, Wisconsin 53706, and the Department of Pharmacological Sciences, School of Medicine, State University of New York at Stony Brook, Stony Brook, New York 11794-8651 (C.C.M.)*

Received December 22, 1995; Accepted March 1, 1996

## SUMMARY

The interactions between β-adrenergic receptor (βAR) antagonists and the $\beta_2$AR were studied with the use of photoaffinity labels. A proteolytic map of the receptor was made and confirmed through amino-terminal amino acid sequencing by locating sites of derivatization. [$^{125}$I]Iodoazidothiophenylalprenolol (IAPTA) is a photoaffinity derivative of the βAR antagonist alprenolol with a photoactivatable group on the aryloxy end of the molecule. IAPTA exclusively derivatizes a peptide consisting of transmembrane domains (TMs) 6 and 7 of the hamster lung $\beta_2$AR, supporting the contention that TMs 6 and 7 interact with the aryloxy portion of the βAR antagonist pharmacophore. The βAR antagonist photoaffinity labels [$^{125}$I]iodoazidobenzylpindolol (IABP), [$^{125}$I]iodoazidophenyl CGP-12177A (IAPCGP), and [$^{125}$I]iodocyanopindololdiazarene (ICYPdz) are similar in that their photoactive moieties are attached to the amino end of the antagonist pharmacophore. IABP derivatized TMs 5-7 and a peptide containing TM 1 to approximately equal extents. IAPCGP derivatized TMs 6 and 7 ≫ TM 5 = TM 4 = TMs 2 and 3 = TM 1. ICYPdz derivatized TM 1 ≫ TMs 6 and 7 > TM 4. We conclude that the aryloxy end of the βAR antagonist pharmacophore is highly constrained within TMs 6 and 7, whereas the amino terminus is much less constrained and able to assume multiple conformations. Molecular dynamics simulations predict that IABP, IAPCGP, and ICYPdz favor a folded conformation, with both ends close together. Derivatization of TMs 6 and 7 by IABP, IAPCGP, and ICYPdz suggests the folded conformation of these compounds in the ligand binding pocket.

βAR antagonists are used extensively to treat cardiovascular disorders. A large collection of βAR antagonists have been synthesized that bind to the receptor with high affinity but, unlike agonists, they do not enable the receptor to activate the heterotrimeric G protein $G_s$. So far, three pharmacologically distinct subtypes of βAR ($\beta_1$, $\beta_2$, and $\beta_3$) have been identified (1-3). All are members of the superfamily of seven-TM, G protein-coupled receptors (for a review, see Ref. 4).

The ligand binding site of the $\beta_2$AR has been extensively characterized through the use of a variety of techniques (5); deletion mutations (6), fluorescence probe analysis (7), and photoaffinity labeling experiments (8, 9) have indicated that the ligand binding site lies within the TMs of the receptor. Point mutations of the hamster lung $\beta_2$AR have revealed a key amino acid residue in TM 3 ($Asp^{113}$) that is essential for high affinity binding of both agonists and antagonists (10), as well as residues in TM 5 ($Ser^{204}$ and $Ser^{207}$) that are critical for agonist activation of the receptor (11). As a result of these studies, a model has evolved with regard to the interactions between the basic βAR agonist pharmacophore, consisting of an alkylamine, β-hydroxyl, and catechol hydroxyls, and the receptor.

Less clear at the present time, however, is the disposition within the binding pocket of the bulky aryloxy and alkylamine moieties common to all high affinity βAR antagonists. It has been proposed that the addition of a hydrophobic group to the amino end of the βAR ligand pharmacophore can result in molecules that are capable of existing in either a folded (both ends closed together) or extended conformation in space (12). Recently, Blin *et al.* (13) used molecular dynamics modeling to analyze the three-dimensional structures of compounds such as pindolol, cyanopindolol, and CGP-12177A (4-(3-(p-azido-m-iodophenyl)-2-hydroxypropoxy)-benzimidazol-2-one) with antagonist activity at $\beta_1$AR and $\beta_2$AR and partial agonist activity at $\beta_3$AR. They concluded that these

This work was supported by a Pharmaceutical Manufacturers' Association predoctoral fellowship (G.H.H.) and National Institutes of Health Grant GM33138 (A.E.R.).

[1] Current affiliation: Department of Pharmacology, University of Washington, Seattle, Washington 98195.

**ABBREVIATIONS:** βAR, β-adrenergic receptor; TM, transmembrane domain; IAPTA, [$^{125}$I]iodoazidothiophenylalprenolol; IABP, [$^{125}$I]iodoazidobenzylpindolol; IAPCGP, [$^{125}$I]iodoazidophenyl CGP-12177A; ICYPdz, [$^{125}$I]iodocyanopindololdiazarene; PMSF, phenylmethylsulfonyl fluoride; PVDF, polyvinylidine difluoride; SDS, sodium dodecyl sulfate; PAGE, polyacrylamide gel electrophoresis; ICYP, [$^{125}$I]iodocyanopindolol; DDT, dithiothreitol; Con-A, concanavalin-A; TPCK, *N*-tosyl-L-phenylalanine chloromethyl ketone; pBABC, *para*-bromoacetylbenzylcarazolol.

compounds are capable of adopting either extended or folded conformations and proposed that the folded conformation is in large part responsible for their $\beta_1/\beta_2$ antagonist activity, whereas the extended conformation is responsible for the $\beta_3$ agonist activity.

In the current study, we used the novel photoaffinity label IAPTA (Fig. 1), with a photoactive group on the aryloxy end of the antagonist pharmacophore to probe the interactions of this antagonist region with the purified hamster $\beta_2$AR. We show that IAPTA photoaffinity labeling of purified hamster $\beta_2$AR exclusively derivatized a peptide containing TMs 6 and 7. To assess the disposition of antagonist alkylamine groups within the $\beta_2$AR, we studied the photoaffinity labeling of the purified hamster $\beta_2$AR by photoactivatable derivatives of pindolol (IABP), cyanopindolol (ICYPdz), and CGP-12177A (IAPCGP) (Fig. 1). These photoaffinity labels contain aromatic rings at both ends of the $\beta$AR ligand pharmacophore,

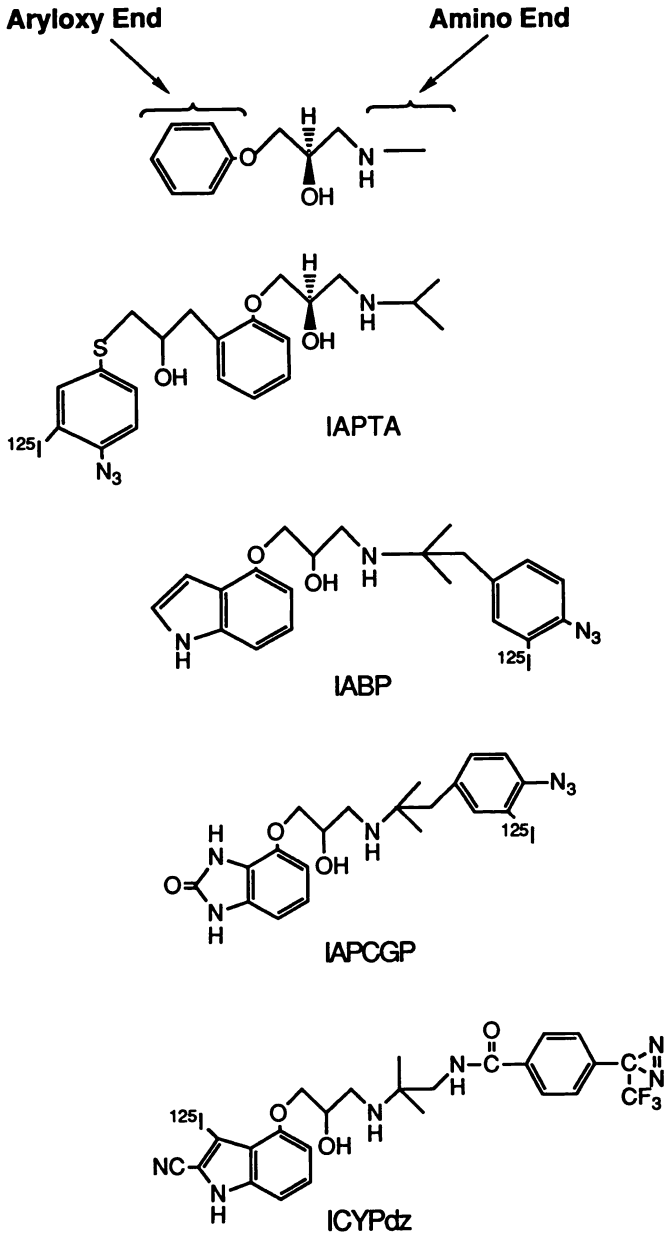


**Fig. 1.** Structures of the photoaffinity labels IABP, IAPCGP, ICYPdz, and IAPTA.

and molecular dynamics simulations indicated a strong preference for the folded conformation for all three ligands. Because the photoactivatable group in all three of these compounds is on the amino end of the pharmacophore, the folded conformations of the photolabels, if present in the ligand binding site, should derivatize the same sites within the receptor as IAPTA. We show here that IABP, IAPCGP, and ICYPdz each specifically labeled TMs 6 and 7 as well as a distinct set of other receptor peptides.

## Materials and Methods

**Chemicals.** (±)-ICYPdz and [$^{125}$I]NaI were purchased from Amersham (Arlington Heights, IL). Thallium trichloride was purchased from Curtin Matheson Scientific (Houston, TX). The epoxide 2,3-epoxypropoxybenzimidazole-2-one was a gift from Ciba-Geigy Corp. (Basel, Switzerland). Receptor-grade digitonin was obtained from Gallard Schlesinger (Carla Place, NJ). Sepharose 4B, (−)-alprenolol-(+)-tartrate, Sephadex G-50, soybean trypsin inhibitor, TPCK-treated trypsin (EC 3.4.21.4)], *Staphylococcus aureus* V-8 protease (EC 3.4.21.19), and all antibiotics were purchased from Sigma Chemical Co. (St. Louis, MO). Leupeptin was obtained from Peptides International (Louisville, KY). Coomassie brilliant blue, 3-cyclohexylamino-1-propanesulfonic acid, 2-mercaptoethanol, PMSF, chloroform, acetonitrile, triethylamine, and $\alpha$-D-methylmannoside were purchased from Aldrich Chemical Co. (Milwaukee, WI). Con-A/agarose was obtained from Vector Labs (Burlingame, CA). Ex-Cell 400-defined medium was purchased from JR Scientific (Woodland, CA). Aldehyde-free glacial acetic acid was obtained from Baker Chemical (Phillipsburg, NJ). Sequencing grade PVDF membrane, acrylamide, bisacrylamide, and ammonium persulfate were purchased from Bio-Rad (Hercules, CA). *N,N,N′N′*-Tetramethylethylenediamine was obtained from Boerhringer Mannheim Biochemicals (Indianapolis, IN). SDS was purchased from Bethesda Research Labs (Gaithersburg, MD), and Sf-9 cells were obtained from American Type Culture Collection (Rockville, MD).

**Synthesis of photolabels.** IABP was synthesized according to the method of Rashidbaigi and Ruoho (14). IAPCGP was synthesized with the same method using the epoxide 2,3-epoxypropoxybenzimidazole-2-one in the place of 1-(4-indoloxy)-2,3-epoxypropane. The epoxide was reacted with [$^{125}$I]-1-(4-azido-3-iodophenyl)-2-methyl-2-propylamine for 4 days at 60°. The product was purified through silica gel thin layer chromatography (20 cm × 10 cm × 0.25 mm plate) in 90:10:1 chloroform/acetonitrile/triethylamine, visualized with the use of autoradiography, and extracted from silica gel with ethanol (50% yield). The product was radiopure as assessed with silica gel thin layer chromatography in 90:10:1 chloroform/acetonitrile/triethylamine. IAPTA was synthesized as previously described (15).

**Synthesis of alprenolol/Sepharose affinity chromatography resin.** Sepharose 4B was derivatized with (−)-alprenolol according to a modification of the method of Caron *et al.* (16). In the final step, the incubation with 1% $NaBH_4$ was omitted. Instead, the gel was resuspended in 1.5 volumes of 10 mM DTT and 50 mM sodium phosphate, pH 8.0, and stirred for 1 hr at an ambient temperature. The DTT-containing buffer was removed, and the gel was washed with 10 volumes of water. The gel was then suspended in 1.5 volumes of 11 mM iodoacetamide and 50 mM sodium phosphate, pH 8.0, and stirred for 3 hr. The iodoacetamide-containing buffer was removed, and the gel was washed with 15 volumes of water. The gel was resuspended in 1 volume of 0.02% $NaN_3$ and stored at 4° until use.

**Cell culture and receptor solubilization.** The *Spodoptera frugiperda*-derived cell line (Sf-9) was cultured in Ex-Cell 400-defined medium containing 2.5 $\mu$g/ml gentamicin, 2.5 $\mu$g/ml streptomycin, and 2.5 units/ml penicillin G. Cells were maintained in monolayer culture at 28° in sealed T-flasks and subcultured every 2-3 days. Cells were grown in 0.5 liter of suspension culture before preparative infection with the receptor-encoding baculovirus. Suspension cul-

tures were initiated at 500,000 cells/ml and grown in a sealed 1-liter flask at 28°. When the 0.5 liter of suspension cultures had reached a density of >1 million cells/ml, it was infected with the receptor-encoding baculovirus (17) at a multiplicity of infection of 0.2-0.4. At 2-4 days after infection, the cells were collected through centrifugation at 300 × *g* for 15 min at 4°. The cells were resuspended in 100 ml of 1% digitonin, 100 mM NaCl, 10 mM Tris·HCl, pH 7.4, 2 mM EDTA, 1 mM PMSF, 10 μg/ml leupeptin, and 10 μg/ml soybean trypsin inhibitor and stirred at 4° for 1 hr. The suspension was then centrifuged at 48,000 × *g* for 20 min at 4°.

**Soluble receptor binding assay.** The 1.0% digitonin extract was diluted to 0.05% in digitonin with 100 mM NaCl, 10 mM Tris·HCl, pH 7.4. To 300 μl of the diluted extract we added ICYP to a final concentration of ~0.5 nM. The sample was incubated at 30° for 30 min, and then 200 μl of the sample was gently pipetted onto a 3.5 ml Sephadex G-50 column (10 × 0.7 cm; Bio-Rad Econo-column) that had been equilibrated in LD buffer (0.05% digitonin, 100 mM NaCl, 10 mM Tris·HCL, pH 7.4, and 2 mM EDTA). The column was eluted with 1.8 ml of LD buffer, of which the final 1 ml was collected. The assay was also performed in the presence of 10 μM (−)-alprenolol to define nonspecific binding. The bound ICYP eluting in the void volume was quantified with a Packard 800C γ counter.

**Alprenolol/Sepharose chromatography.** The digitonin extract of infected Sf-9 cells (100 ml) was chromatographed on (−)-alprenolol/Sepharose. The (−)-alprenolol/Sepharose was packed in a Pharmacia 40 × 2.5 cm column, the column was equilibrated with 2 volumes of LD buffer, and the extract was loaded on the column at 3 ml/min. The column was at ambient temperature and the sample was on ice during loading. The column was washed with 3 volumes of 0.5% digitonin, 0.5 M NaCl, 50 mM Tris·HCl, pH 7.4, and 2 mM EDTA. The column was next washed with 2 volumes of LD buffer. The column was eluted with a linear, 0-400 μM (−)-alprenolol gradient in 4 volumes of LD buffer. The gradient elution was collected in 20-ml fractions. The fractions were placed on ice immediately after collection. At the end of the gradient, the column was washed with an additional 1 column volume of LD buffer, which was collected in 20-ml fractions. The fractions were assayed for ICYP binding activity, as described above.

**Con-A/agarose chromatography.** Con-A/agarose (150 μl; 6 mg lectin/ml) was washed twice with LLD buffer (1 ml of 0.02% digitonin, 150 mM NaCl, 10 mM Tris·HCl, pH 7.4) in a 1.5-ml Eppendorf tube. Affinity-purified receptor concentrate was added (300 pmol; 1.2 ml), and the suspension was tumbled at 4° for 1 hr. The suspension was centrifuged at 2000 × *g* for 5 min in a Beckman Microfuge, and the supernatant was removed. The pellet was resuspended and washed three times with 1 ml of LLD buffer. The Con-A/agarose was then resuspended in 0.5 ml of 200 mM α-D-methylmannoside in LLD buffer and tumbled at 4° for 10 min. The suspension was centrifuged as before, and the supernatant removed and stored at 4°. The Con-A/agarose was washed with an additional 0.5 ml of 200 mM α-D-methylmannoside in LLD buffer. The supernatant was removed and pooled with the first α-D-methylmannoside fraction. ICYP binding assays of the various fractions was performed as described above.

**Photoaffinity labeling of purified receptor.** The free alprenolol was removed from affinity-purified $\beta_2$AR through chromatography over a G-50 column as described previously. IABP (in ethanol) was added to receptor-containing solutions to give the indicated concentrations, leaving a final ethanol concentration of ≤2%. Alprenolol (10 μM) was added to some samples for assessment of nonspecific labeling. The solutions were incubated at 30° for 45 min and then photolyzed for 5 sec at 4° with an AH6 high pressure mercury lamp at a distance of 10 cm.

**Tryptic time course of photolabeled $\beta_2$AR.** TPCK-treated trypsin was added to photolabeled receptor solutions to a final concentration of 1 μg/ml, and the solutions were incubated at 30°. At indicated times, aliquots (100-200 μl) were removed, and the proteolysis was terminated with the addition of 5 μg of soybean trypsin inhibitor. Samples were routinely frozen and stored at −20° until they were analyzed with SDS-PAGE on 0.75-mm 10-18% polyacrylamide gradient gels according to the system of Fling and Gregerson (18).

**Preparation of tryptic peptides for sequence analysis.** Affinity-purified $\beta_2$AR (200 pmol; 0.8 ml) was photoaffinity labeled with IABP (5.5 nM) as described previously. The labeled receptor was combined with 1 nmol of affinity-purified $\beta_2$AR and incubated with 150 μl of Con-A/agarose for 80 min at an ambient temperature with stirring. After centrifugation for 5 min in a Beckman microfuge, the supernatant was removed. The Con-A/agarose was washed three times with LLD buffer. The Con-A/agarose was next incubated with 1 ml of 50 mM α-methylmannoside in LLD buffer for 5 min at ambient temperature. The supernatant was removed, and the Con-A/agarose was washed with an additional 1 ml of 50 mM α-methylmannoside. Half of the second α-methylmannoside LLD fraction was pooled with the entire first α-methylmannoside fraction (~1.5 ml total). TCPK-treated trypsin (3 μg; 36 units) was added to the pooled α-methylmannoside LLD fractions, and the solution was incubated at an ambient temperature for 48 hr. Proteolysis was terminated by the addition of PMSF (1 mM final concentration). The solution was concentrated to 100 μl with an Amicon Centricon 3 ultrafiltration device (centrifuged for 3 hr at 6800 × *g* at 4°).

**Preparative SDS-PAGE of tryptic peptides and transfer to PVDF membrane.** The method of Fling and Gregerson (18) was used with the following modifications. In all cases, the SDS used was recrystallized according to the method of Hunkapiller *et al.* (19). The glycerol used in the sample buffer was of analytical grade. The polymerized, resolving gel was aged for 8 hr and the stacking gel was aged for 4 hr before use. The resolved peptides were transferred from the polyacrylamide gel to PVDF membrane with the use of 10 mM 3-cyclohexylamino-1-propanesulfonic acid, pH 11, and 10% methanol in a Hoefer model TE 50 Transphor electrophoresis unit at 70 V for 30 min. The PVDF membrane was stained for 5 min in 0.025% Coomassie blue in 40% methanol and then destained for 15 min in 45% methanol and 10% aldehyde-free acetic acid. The membrane was air dried and subjected to autoradiography with Kodak X-Omat film. The Coomassie blue-stained peptides, which corresponded to radioactive bands on the autoradiogram, were excised from the membrane with a razor blade and subjected to amino-terminal amino acid analysis.

**Purification of IABP-labeled 30-kDa tryptic peptide.** Receptor (100 pmol) was photoaffinity labeled with IABP (0.75 nM) and combined with an additional 1.94 nmol of affinity-purified $\beta_2$AR. To this solution containing 2.04 nmol of $\beta_2$AR, we added 10 μg (120 units) of TPCK-treated trypsin in 10 μl of water. The solution was incubated at an ambient temperature for 20.5 hr, and proteolysis was terminated with the addition of PMSF (1 mM final concentration). The solution was adjusted to 0.05% in recrystallized SDS and divided into six aliquots. Each aliquot was incubated with 150 μl of Con-A/agarose at ambient temperature for 1 hr with stirring and then centrifuged for 5 min in a Beckman Microfuge, and the supernatant was removed. Each Con-A/agarose aliquot was washed three times with 1 ml of LLD buffer and then stirred for 15 min at an ambient temperature with 0.5 ml of 200 mM α-methylmannoside in LLD buffer. The supernatants were removed and pooled. Each aliquot was washed with an additional 0.5 ml of 200 mM α-methylmannoside. The supernatants from this wash were pooled with the first six fractions containing α-methylmannoside, and a small sample (300 μl) was removed for assessment of the purity of the 30-kDa tryptic peptide. The remaining 5.7 ml was concentrated to 2 ml with the use of an Amicon Centricon 30 ultrafiltration device.

**Cleavage of 30-kDa IABP-labeled tryptic peptide with *S. aureus* V-8 protease.** To the 30-kDa peptide prepared as described above (2 ml), we added 100 μg (7 units) of *S. aureus* V-8 protease preparation. The solution was incubated at an ambient temperature for 52 hr. After 100 μl of the solution was removed, the remainder was concentrated to 100 μl with the use of a Centricon 3 ultrafiltration device as described above. The concentrate was lyophilized to dryness and subjected to electrophoresis, and the resolved peptides

were transferred to PVDF membrane as described above. Peptides excised from the destained PVDF membrane were subjected to amino-terminal amino acid sequence analysis.

**Preparation of 4.5-kDa IABP-labeled, V-8-cleaved peptide for radiosequencing.** The IABP-labeled 4.5-kDa peptide was prepared as described above except that 1.11 nmol of $\beta_2$AR was photoaffinity labeled with IABP (2.1 nM) and combined with another 1.66 nmol of affinity-purified $\beta_2$AR. The first four cycles of amino-terminal amino acid sequencing were performed for chemical sequence, and then radiosequencing was continued with 1:1 butyl chloride/ethylacetate as the solvent for the extraction of phenylthiohydantoin amino acid derivatives. The phenylthiohydantoin amino acids from each cycle were collected, and the radioactivity in each cycle was quantified through scintillation counting.

**Con-A/agarose chromatography of V-8-cleaved 30-kDa peptide.** Purified 30-kDa peptide (prepared as described above, 0.5 ml) was chromatographed on 4-ml Sephadex G-50 columns to remove $\alpha$-methylmannoside. The 30-kDa peptide was then cleaved with V-8 protease in a 1-ml volume, as described above. The digest was then subjected to Con-A/agarose chromatography, as described, except that the digest was adjusted to 5 mM dithiothreitol before being incubated with the Con-A/agarose. The polypeptides that were not retained by the Con-A/agarose as well as the polypeptides that were specifically eluted with 200 mM $\alpha$-methylmannoside were subjected to SDS-PAGE on a 10-18% acrylamide gel. The gel was dried, and the radioactive peptides were made visible through autoradiography.

**Quantification of photolabel derivatization of peptides.** Proteolytic digests of labeled receptor were separated with the use of SDS-PAGE as described above. Autoradiographs of the dried gels were made with the autoradiograph as a template, and the gels were cut into strips corresponding to each lane. Each strip was cut into 3-mm slices, and the $^{125}$I in each slice was measured with a Packard 800C $\gamma$ counter.

**Amino-terminal sequence analysis.** Amino-terminal amino acid sequencing was performed directly on samples from PVDF membranes at the Michigan State Macromolecular Structure Facility (East Lansing, MI), using an Applied Biosystems 477A amino acid sequencer.

**Molecular dynamics simulations.** The conformations available to the photoaffinity ligands were simulated with the use of molecular dynamics. A variation of the simulated annealing strategy was used, with high temperature dynamics allowing the molecules to overcome any energy barriers and to sample a large range of conformational space. The dynamics calculations were performed with the Discover 2.9 package (Biosym, San Diego, CA). All simulations were carried out *in vacuo* with Biosym's CVFF force field without charges. The time steps of the dynamics were 1.0 fsec.

The photolabels were built in an extended conformation and subjected to 100 cycles of molecular mechanics to relieve bad contacts. The molecular dynamics simulation was initiated by equilibrating each molecule for 50 psec at 300° K. The temperature in the simulation was then raised to 700° K, and the system was equilibrated for 10 psec at this temperature. The simulation proceeded for 200 psec at 700° K to allow the molecule to sample different conformations. Every 0.5 psec, a conformation was recorded for further analysis. Each of 400 high temperature structures were cooled to 300° K over 1 psec and allowed to relax at the lower temperature for 2 psec. These 400 structures were saved for analysis, and the lowest energy conformation directly accessible to each conformer was determined through molecular mechanics.

## Results

**Purification of hamster lung $\beta_2$AR from Sf-9 cells.** The model in this study was the guinea pig lung $\beta_2$AR (2) expressed in the *Spodoptera frugiperda* cell line Sf-9 via a baculovirus vector. The baculovirus expression system produced ≤10 nmol/0.5 liter of cells, allowing purification on a scale of several hundred micrograms. The affinity of the recombinant receptor for ICYP was measured in Sf-9 cell membranes through equilibrium binding and Scatchard analysis. The recombinant $\beta_2$AR was found to bind ICYP in a saturable and alprenolol-protectable manner with a $K_d$ of 83 pM (data not shown). The $\beta_2$AR expressed in this manner was solubilized with digitonin and purified by affinity chromatography over alprenolol/Sepharose and Con-A/agarose. The purity of the recombinant $\beta_2$AR after alprenolol/Sepharose chromatography was assessed with the use of saturation ICYP binding and quantification of the amount of protein according to the method of Peterson (20) or of Schaffner and Weissmann (21). The specific ICYP binding activity of the affinity-purified $\beta_2$AR determined with these methods ranged from 5.5 to 8.3 nmol receptor/mg protein, indicating that the purity of the preparations was 30-45%. The yields at this step ranged from 40% to 70%. The purity of $\beta_2$AR preparations after both alprenolol/Sepharose chromatography and Con-A/agarose chromatography was assessed through Coomassie blue staining of samples subjected to SDS-PAGE. Preparations eluted from Con-A/agarose by $\alpha$-methylmannoside migrated as a single-stained species with an apparent molecular mass of 53 kDa (Fig. 2A, *lane 1*), which is consistent with the original description of Sf-9 cell/baculovirus-expressed receptor (17).

**Peptide mapping of purified $\beta_2$AR with trypsin and V-8 protease.** The purified receptor (molecular mass, 53 kDa; Fig. 2A, *lane 1*) was cleaved with trypsin (2 $\mu$g/ml for 48 hr at an ambient temperature). After this treatment, receptor peptides of 20-kDa and 8-kDa peptides were visible after SDS-PAGE, electroblotting to PVDF membranes, and Coomassie blue staining (Fig. 2A, *lane 2*) along with trypsin (24 kDa). The Coomassie blue-stained 20-kDa and 8-kDa peptides were excised from the membrane and subjected to amino-terminal sequence analysis directly from the PVDF. Analysis of the 8-kDa tryptic $\beta_2$AR peptide (Fig. 2A, *lane 2*) revealed the amino-terminal sequence as $H_2$N-S G K F Y L K E (Fig. 2B), corresponding to residues 261-268 of the hamster lung $\beta_2$AR (2). The cDNA sequence, however, indicates a serine at position 262 and a cysteine at position 265. The misreading of Ser$^{262}$ as glycine may be due to glycine contamination and trailing of serine from the previous cycle. The misreading of Cys$^{265}$ as tyrosine could be due to derivatization of the cysteine sulfhydryl during purification of the 8-kDa peptide. The sequence suggests cleavage of the receptor by trypsin at the carboxyl-terminal side of Arg$^{260}$. The apparent molecular mass and amino-terminal sequence identify a tryptic fragment that includes TMs 6 and 7 and a probable carboxyl-terminal cleavage site for trypsin at either Arg$^{343}$ or Arg$^{344}$ (Fig. 3).

Analysis of the 20-kDa peptide indicated an amino-terminal sequence of $N_2$H-D V T E X X D E A X V V G M A I L M S V, corresponding to residues 23-42 of the hamster lung $\beta_2$AR. Cleavage occurred on the carboxyl-terminal side of His$^{22}$. Less extensive tryptic cleavage of the receptor (5 $\mu$g trypsin/nmol $\beta_2$AR, 20.5 hr at 30°) resulted in an additional peptide of 30 kDa. The 30-kDa tryptic fragment bound to, and was specifically eluted from, Con-A/agarose, reflecting the presence of *N*-glycosylation. This character was exploited to purify the 30-kDa peptide from all other tryptic fragments of the receptor (Fig. 2A, *lane 3*).

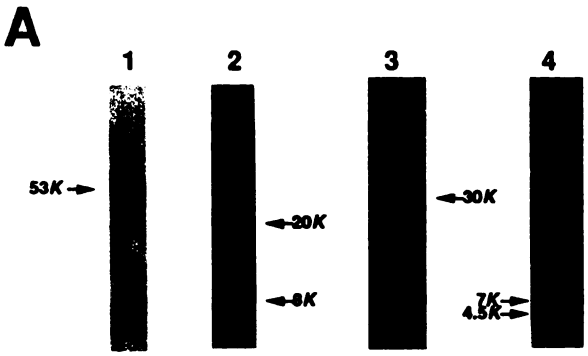


B

**Tryptic Peptides**

*8K* SGKFYLKE

*20 K* DVTEXXDEAXVVGMAILMSV

**V-8 Peptides**

*4.5 K* TCCDFFTNQAYAIASSIVSFYVPL VIMVFVSRVFQVAKRQ

*7 K* TLXVIAVDRYIA

**Fig. 2.** Tryptic and V-8 protease peptides of the $\beta_2$AR. A, *Lane 1*, Coomassie blue staining of 75 pmol (4 $\mu$g) of receptor purified through sequential alprenolol/Sepharose and Con-A/agarose chromatography and resolved with the use of SDS-PAGE on a 12% polyacrylamide gel. *Lane 2*, purified receptor (1.2 nmol; 64 $\mu$g) was cleaved with trypsin, resolved with the use of SDS-PAGE on a 10-20% polyacrylamide gradient gel, transferred to PVDF membrane, and stained with Coomassie blue. *Lane 3*, purified 30-kDa tryptic peptide (4 $\mu$g) was resolved with the use of SDS-PAGE on a 10-20% polyacrylamide gradient gel and stained with Coomassie blue. *Lane 4*, Purified 30-kDa tryptic peptide (30 $\mu$g) was cleaved with V-8 protease, resolved with the use of SDS-PAGE on a 10-20% acrylamide gradient gel, transferred to PVDF membrane, and stained with Coomassie blue. B, Amino-terminal sequences of the tryptic and V-8 protease peptides of the $\beta_2$AR.

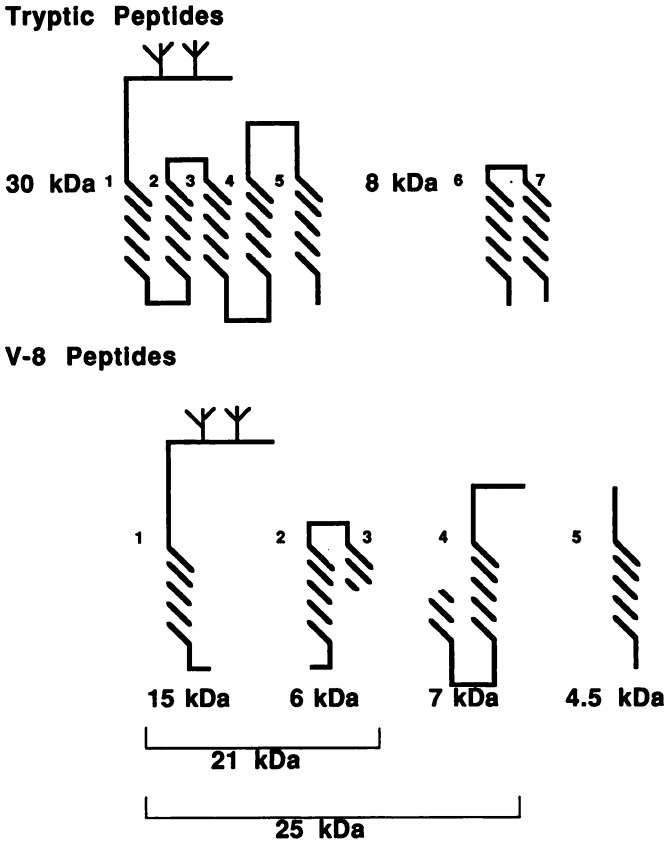


**Fig. 3.** Summary of tryptic and V-8 protease peptides of the $\beta_2$AR. *Bundles of diagonal lines*, membranes spanning helices (numbered from amino to carboxyl terminal). *Branched lines on the amino-terminal tail*, sites of *N*-linked glycosylation. The molecular mass was determined with SDS-PAGE for each peptide (in kDa).

The purified 30-kDa peptide was further cleaved with *S. aureus* V-8 protease, yielding two peptides of 4.5 and 7 kDa (Fig. 2A, *lane 4*). Analysis of the 4.5-kDa peptide established the amino-terminal 41-amino acid sequence to be $H_2N$-T C C D F F T N Q A Y A I A S S I V S F Y V P L V I M V F V Y S R V F Q V A K R Q, corresponding to residues 189-229. The 4.5-kDa fragment includes all of TM 5 of the hamster lung $\beta_2$AR (Fig. 3). The sequence is consistent with cleavage of the receptor at $Glu^{188}$. This experiment was repeated four times with equivalent results. These data suggest that the 30-kDa tryptic peptide includes TMs 1-5 (Fig. 3). Under the conditions used, the preferred site of tryptic cleavage is between TMs 5 and 6, not between TMs 4 and 5 as reported previously (22).

The amino-terminal sequence of the 7-kDa peptide was established as $H_2N$-T L X V I A V D R Y I A, corresponding to residues 123-134 of the hamster lung $\beta$AR. The sequence suggests cleavage of the receptor on the carboxyl-terminal side of $Glu^{122}$ by V-8 protease. Under the conditions used, V-8 protease selectively cleaves at glutamyl bonds. Both peptides that were sequenced were cleaved at glutamyl bonds although they also contained aspartyl bonds that were not cleaved. The amino-terminal sequence and size of the 7-kDa peptide, as well as the known V-8 protease cleavage as $Glu^{188}$, identify a fragment composed of residues 123-188, the carboxyl-terminal third of TM 3 and all of TM 4 (Fig. 3).

The identities of the 8-kDa tryptic peptide as well as 4.5- and 7-kDa fragments of the 30-kDa tryptic peptide were established through amino-terminal sequence analysis. Other V-8 protease digest products of the 30-kDa peptide, whose identity could not be confirmed through amino-terminal sequence analysis, can be readily identified. V-8 protease is selective for $Glu^X$ over $Asp^X$ bonds under any condition and under some conditions will exclusively cleave glutamate. Under the conditions that we used (0.02% digitonin, 150 mM NaCl, 10 mM Tris·HCl, pH 7.4), $Glu^X$ bonds are cleaved preferentially as both the 7- and 4.5-kDa peptide displayed uncleaved $Asp^X$ bonds in their sequences. If cleavage occurred only at $Glu^X$ bonds, there are only five cleavage sites possible in the 30-kDa peptide. The first is $Glu^{167}$, generating the 4.5-kDa peptide. The second is $Glu^{122}$, generating the 7-kDa peptide. These cleavages were confirmed through sequence analysis of the peptides. The third cleavage site is $Glu^{107}$, which would give rise to a 14-amino acid peptide from TM 3. Cleavage at this site, however, seems unlikely as the bond is a glutamate-phenylalanine bond, which is cleaved at a lesser rate than other $Glu^X$ bonds (23). The fourth possible site is $Glu^{62}$, generating a 6-kDa peptide, consisting of TMs 2 and 3 (assuming no cleavage at $Glu^{107}$) as well as a glycosylated 15-kDa peptide consisting of TM 1 and the amino terminus. The fifth site is $Glu^{30}$, releasing the amino terminus and *N*-linked carbohydrate; however, no evidence for cleavage at

Glu[30] was detected. The observed cleavage sites are outlined in Fig. 3.

**Peptide mapping of IAPTA-labeled $\beta_2$AR.** IAPTA labeling of the $\beta_2$AR was completely protectable with the use of 10 μM (−)-alprenolol (Fig. 4, *lanes 1 and 2*). At 1 hr (Fig. 4, *lane 5*) after the addition of trypsin, the receptor was largely cleaved to a 23-kDa radioactive peptide that was subsequently cleaved, after 16 hr, to an 8-kDa radioactive fragment (Fig. 4, *lane 6*). The 30-kDa tryptic peptide containing TMs 1-5 was not labeled to a significant extent. The exquisite selectivity of IAPTA photolabeling for the 8-kDa tryptic peptide made up of TMs 6 and 7 suggests that the aryloxy portion of this alprenolol derivative is highly constrained within this region of the receptor.

**Peptide mapping of IABP-labeled $\beta_2$AR.** IABP was shown to specifically label the partially purified, digitonin-dispersed receptor (Fig. 5A, *lanes 1 and 2*). Time courses for digestion with trypsin of IABP-labeled $\beta_2$AR (Fig. 5A, *lanes 3 and 4*) revealed a radioactive 30-kDa fragment that was resistant to further cleavage. IABP was also found to label a 23-kDa intermediate fragment (not shown) that was cleaved subsequently to an 8-kDa peptide. The two peptides displayed a 2:1 labeling ratio, favoring the 30-kDa peptide. As detailed above, the 30-kDa peptide is the amino terminus including TM 5, and the 8-kDa peptide is TMs 6 and 7.

On Con-A/agarose chromatography in the presence of SDS, the 30-kDa peptide was retained, whereas the 8-kDa peptide was not, indicating that the 30-kDa peptide was glycosylated. The purified, IABP-labeled 30-kDa peptide (Fig. 5A, *lanes 5 and 6*) was cleaved subsequently by V-8 protease. This protease cleaves the 30-kDa-labeled peptide into radiolabeled peptides of 25, 21, 15, and 4.5 kDa (Fig. 5A, *lanes 7 and 8*). These peptides are all site-derived, specifically labeled peptides, as 10 μM (−)-alprenolol suppressed photolabeling of all four receptor fragments (Fig. 5A, *lanes 2, 4, 6, and 8*). Thus, IABP derivatizes TM 5 (4.5-kDa peptide). Radiosequencing of the 4.5-kDa IABP-labeled peptide revealed a single peak of radioactivity, released at cycle 19. This position corresponds to Ser[207] of the hamster lung $\beta_2$AR (Fig. 5B). Approximately 50% of the radioactivity that was incorporated by IABP into the 30-kDa tryptic peptide was in the 4.5-kDa peptide (TM 5).

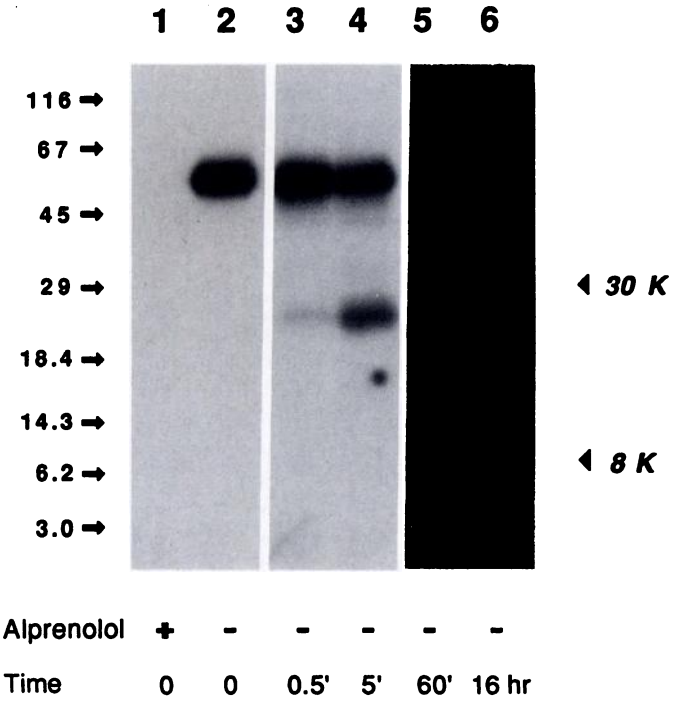


**Fig. 4.** Tryptic time course on IAPTA-labeled $\beta_2$AR. $\beta_2$AR (10 pmol in 1 ml) was photolabeled with IAPTA (0.1 nM); trypsin (1 mg/ml) was added; and the solution was incubated at 30°. At 0 min (*lane 2*), 0.5 min (*lane 3*), 5 min (*lane 4*), 1 hr (*lane 5*), and 16 hr (*lane 6*) after the addition of trypsin, 100-ml samples were removed, and soybean trypsin inhibitor (5 mg) was added. *Lane 1*, $\beta_2$AR photolabeled with IAPTA in the presence of 10 μM (−)-alprenolol. *Numbered arrows on the left*, position of molecular mass standards (in kDa).

Con-A/agarose chromatography of the V-8 protease digests of the 30-kDa IABP-labeled tryptic fragment was performed to determine whether any or all of the 25-, 21-, and 15-kDa fragments contained *N*-linked carbohydrate. The heavily radiolabeled 4.5-kDa peptide was not retained by the lectin in the presence of 0.05% SDS and 5 mM DTT. The larger 25-, 21-, and 15-kDa radiolabeled peptides were all retained by the lectin and eluted with 200 mM α-methylmannoside, establishing the presence of carbohydrate on each peptide (data not shown). Because the *N*-linked glycosylation is proximal to the amino terminus, the 25-, 21-, and 15-kDa peptides are likely successive cleavage products of the 30-kDa peptide by V-8 protease at Glu[167], Glu[122], and Glu[62], respectively. The size and carbohydrate content of the 15-kDa peptide are consistent with proteolytic cleavage at Glu[62], with IABP derivatization at TM 1 (Fig. 3). The derivatization of TMs 5-7 by IABP is consistent with the results of Wong *et al.* (8), who labeled the turkey erythrocyte βAR with IABP and determined that tryptophan 330 in TM 7 was derivatized as well as an undetermined site or sites in TMs 3-5.

The results indicate that IABP, in contrast to IAPTA, labels both TMs 6 and 7 and TMs 1-5. The position of the photolabel in the amino end of the antagonist molecule may place it in a position to react with both sides of the receptor binding pocket. To examine this point further, we mapped the sites of covalent labeling of two additional antagonists with photolabels in the amino end of the molecule.

**Peptide mapping of IAPCGP- and ICYPdz-labeled $\beta_2$AR.** IAPCGP (2.0 nM) labeling of $\beta_2$AR was protectable with 10 μM (−)-alprenolol (Fig. 6A, *lanes 1 and 2*). At 16 hr after the addition of trypsin (Fig. 6A, *lanes 3 and 4*), the receptor was cleaved to two prominent radioactive peptides of 8 and 30 kDa. The ratio of radioactivity covalently bound to the 30- and 8-kDa peptides by IAPCGP was found to be 1:2. Thus, IAPCGP photolabels TMs 6 and 7 preferentially over TMs 1-5. Cleavage of the IAPCGP-labeled, 30-kDa tryptic peptide with V-8 protease resulted in radiolabeled peptides of 25, 21, and 15 kDa (see above and Fig. 3), as well as 7, 6, and 4.5 kDa (Fig. 6A, *lanes 5 and 6*), with the radioactivity distributed equally among all of the peptides.

ICYPdz labeling of the receptor was completely protectable with the use of 10 μM (−)-alprenolol (Fig. 6B, *lanes 1 and 2*). At 16 hr after the addition of trypsin, the receptor was cleaved to a 30-kDa radioactive peptide and an 8-kDa radioactive peptide (Fig. 6B, *lanes 3 and 4*). The ratio of radiolabel covalently bound to the 30- and 8-kDa peptides by ICYPdz was established as 3:1, respectively. Thus, ICYPdz photolabels sites in TMs 1-5 preferentially over TMs 6 and 7. V-8 cleavage of ICYPdz-labeled 30-kDa tryptic peptide resulted in specifically radiolabeled peptides of 25, 21, and 15 kDa (see above and Fig. 3) and 7 kDa (Fig. 6B, *lanes 5 and 6*). The

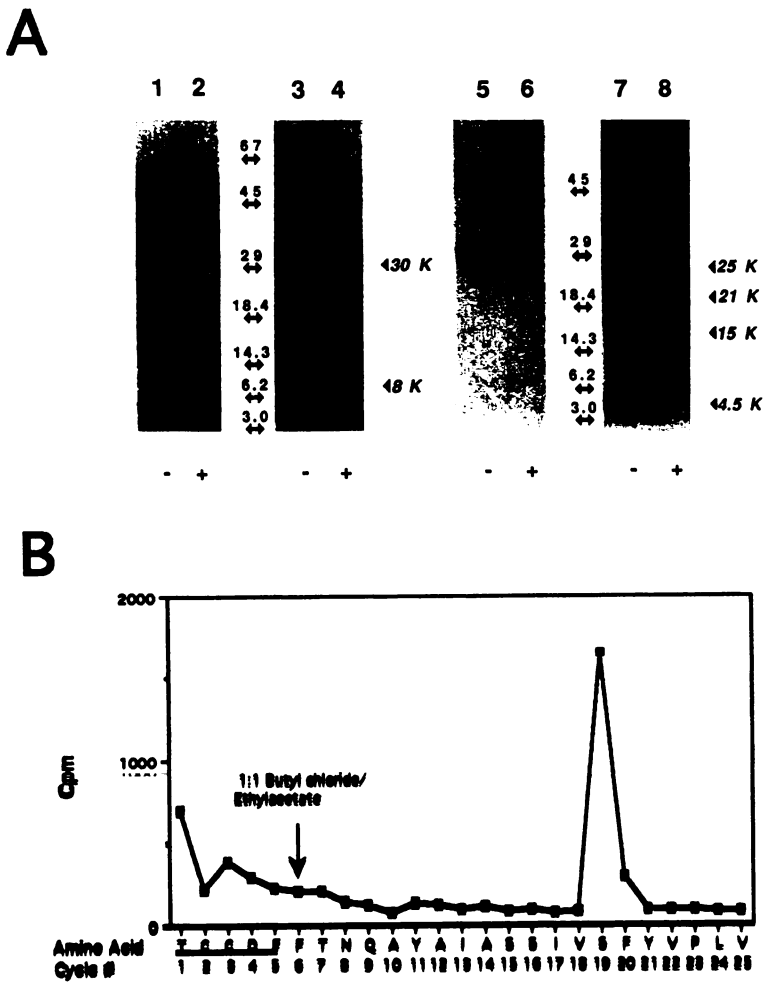


**Fig. 5.** Specificity of IABP photolabeling of the $\beta_2$AR, tryptic peptides, and V-8 protease peptides and radiosequencing of IABP-labeled 4.5-kDa peptide A. Affinity-purified $\beta_2$AR (150 pmol) was photolabeled with IABP (0.5 nM) in the absence (−) or presence (+) of 10 $\mu$M (−)-alprenolol. *Lanes 1 and 2*, uncleaved receptor. *Lanes 3 and 4*, trypsin-cleaved receptor (1 $\mu$g/ml trypsin for 16 hr at 30°). *Lanes 5 and 6*, purified 30-kDa tryptic fragment. *Lanes 7 and 8*, V-8 protease cleavage products (7 units in 2 ml for 52 hr at ambient temperature) of the purified 30-kDa tryptic fragment. Autoradiogram of an SDS-PAGE gel. B, IABP-labeled 4.5-kDa peptide (see Fig. 2B) prepared as described in Materials and Methods except that 1.11 nmol of $\beta_2$AR was photoaffinity labeled with IABP (2.1 nM) and combined with another 1.66 nmol of affinity-purified $\beta_2$AR. The first five cycles of amino-terminal amino acid sequencing were chemically analyzed to confirm the identity of the peptide; then, sequential cleavage was continued with 1:1 butyl chloride/ethylacetate as the solvent. The entire cleavage products from cycles 6-25 were collected, and the radioactivity in each cycle was quantified through scintillation counting.

25-, 21-, and 15-kDa peptides, as a group, were preferentially radiolabeled at a ratio of 10:1 with respect to the 7-kDa peptide.

**Summary of IAPTA, IABP, IAPCGP, and ICYPds insertion sites.** A summary of the results detailed above is given in Table 1. IAPTA labels TMs 6 and 7 exclusively. IABP labels TM 5, TMs 6 and 7, and peptides of 25, 21, and 15 kDa. As discussed above, the larger, glycosylated peptides (25, 21, and 15 kDa) correspond to the amino-terminal fragments of the 30-kDa tryptic peptide cleaved at $Glu^{167}$, $Glu^{122}$, and $Glu^{62}$, respectively. Because IABP does not label TM 4 or TMs 2 and 3, all of the radioactivity incorporated into the 25-, 21-, and 15-kDa peptides is due to labeling of TM 1. Labeling of these three sites by IABP was approximately equal. The major sites of derivatization by IAPCGP were TMs 6 and 7, whereas TMs 1, 4, and 5 and a 6-kDa peptide were labeled to lesser extents. According to the identification of peptides described above, the 6-kDa peptide labeled by IAPCGP corresponds to TMs 2 and 3 (amino acids 63-122). In contrast to IABP and IAPCGP, the major site of ICYPds derivatization was TM 1, with TMs 6, 7, and 4 being minor sites.

## Discussion

Site-directed mutagenesis studies of the $\beta_2$AR have revealed some of the critical binding determinates that interact with agonists and antagonists, as well as the general orientation of these agonists within the receptor. The seven TMs are thought to form a ligand binding pocket with TMs 1 and 7 at the open end and TMs 4-6 at the closed end, analogous to the structure of bacteriorhodopsin (24). The alkyl amine common to both classes of compounds has been shown to interact with $Asp^{113}$ in TM 3 (10), whereas the catechol hydroxyls required for agonist activity are thought to hydrogen bond to $Ser^{204}$ and $Ser^{207}$ in TM 5 (11). These findings lead to the conclusion that agonists are oriented with the amino group toward the open end of the ligand binding pocket near TM 3 and the catechol group toward the closed end near TM 5.

Although $Asp^{113}$ in TM 3 has also been shown to be critical for antagonist binding, several lines of evidence suggest that the aryloxy end of antagonists interacts with TMs 6 and 7 rather than with TM 5, as is the case for agonists. Dixon *et al.* (6) showed that the deletion of TMs 6 and 7 from the $\beta_2$AR resulted in the loss of both agonist and antagonist binding. In addition, Kobilka *et al.* (25), using chimeric $\alpha_2/\beta_2$ adrenergic receptors, demonstrated that TMs 6 and 7 are critical for determination of antagonist specificity. More recently, Suryanarayana and Kobilka (26) showed that high affinity antagonist binding in the $\beta_2$AR is abolished if $Asp^{312}$ in TM 7 of the $\beta_2$AR is mutated to phenylalanine or alanine but is restored if amino acids are substituted that are hydrogen bond donors. They proposed that $Asp^{312}$ forms a hydrogen bond with the aryloxy oxygen of the antagonist pharmacophore. The exclusive labeling of TMs 6 and 7 by IAPTA provides direct evidence that the aryloxy moiety is highly constrained in the

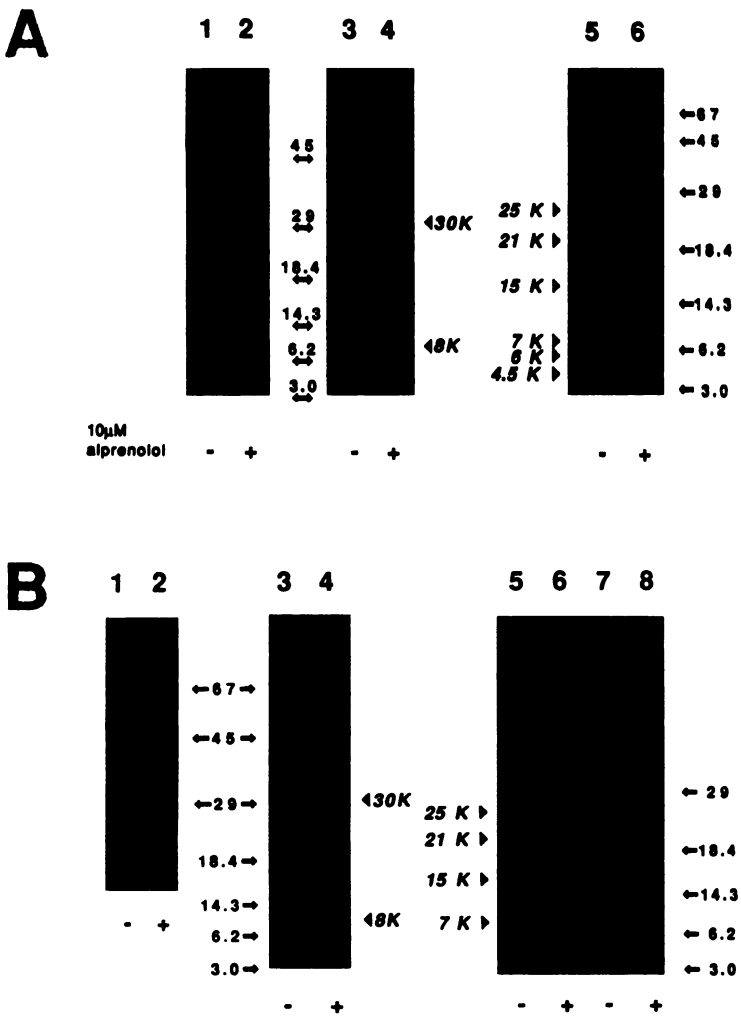


**Fig. 6.** Peptide mapping of IAPCGP- and ICYPdz-labeled $\beta_2$AR. A, *Lanes 1 and 2*, $\beta_2$AR (150 pmol in 1 ml) labeled with IAPCGP (2 nM). *Lanes 3 and 4*, trypsin cleavage of $\beta_2$AR labeled with IAPCGP. *Lanes 5 and 6*, V-8 protease cleavage of Con-A/agarose-purified, IAPCGP-labeled 30-kDa tryptic fragment. Photolabeling was performed in the absence (*lanes 1, 3, and 5*) or presence (*lanes 2, 4, and 6*) of 10 μM (−)-alprenolol. *Numbered arrows*, molecular mass standards (in kDa). B, *Lanes 1 and 2*, $\beta_2$AR (150 pmol in 1 ml) labeled with ICYPdz (1 nM). *Lanes 3 and 4*, trypsin cleavage of $\beta_2$AR labeled with ICYPdz. *Lanes 5 and 6*, V-8 protease cleavage of Con-A/agarose-purified, ICYPdz-labeled 30-kDa tryptic fragment. *Lanes 7 and 8*, Con-A/agarose-purified ICYPdz-labeled 30-kDa tryptic fragment. Photolabeling was performed in the absence (*lanes 1, 3, 5, and 7*) or presence (*lanes 2, 4, 6, and 8*) of 10 μM (−)-alprenolol. *Numbered arrows*, molecular mass standards (in kDa).

TABLE 1

**Summary of the sites and relative intensity of derivatization of the $\beta_2$AR by IAPTA, IABP, IAPCGP, and ICYPdz**

The $^{125}$I content of the photolabeled peptides was determined as described in Materials and Methods.

| Compound | Site of label | Site of derivatization | | | | |
|---|---|---|---|---|---|---|
| | | TM 1 | 2 and 3 | 4 | 5 | 6 and 7 |
| IAPTA | Aryloxy | | | | | ++++ |
| IABP | Alkylamine | ++ | | | ++ | ++ |
| IAPCGP | Alkylamine | + | + | + | + | ++++ |
| ICYPdz | Alkylamine | ++++ | | + | | ++ |

vicinity of TMs 6 and 7 and strong support of the proposal of Suryanarayana and Kobilka (26).

The photolabeling of the receptor by the amino end derivatizing compounds was complex and dependent on the parent antagonist. The multiple sites of receptor derivatization by all three of these probes suggest that the alkylamino groups on these compounds are relatively free for testing of different conformations within the ligand binding site. However, two sites were labeled by all three of these compounds, albeit to differing extents: TM 1 and TMs 6 and 7. The observation that TMs 6 and 7 can be derivatized by IABP, IAPCGP, and ICYPdz as well as IAPTA suggests that IABP, IAPCGP, and ICYPdz can assume folded conformations within the ligand binding site that bring the amino alkyl groups into close proximity to the aryloxy groups and consequently, TMs 6 and 7. Molecular dynamics analysis of IABP, IAPCGP, and ICYPdz indicated lowest energy conformations, with inter-ring distances ranging from 4.0 to 6.5 Å (Fig. 7, A–C). Although these models do not imply that the photolabels must exist in a folded conformation, they make the point that the folded conformation is a potentially favorable one. Indeed, the derivatization of TM 1 by these compounds would be difficult to explain in the context of the folded conformation.

The extent of derivatization of TM 1 varied widely among IABP, IAPCGP, and ICYPdz. IABP and IAPCGP, which are identical in the alkylamine end, derivatized TM 1 to an equal and lesser extent, respectively, than other sites. For ICYPdz, on the other hand, TM 1 was the predominant site of derivatization. The alkylamine structure of ICYPdz, which differs substantially from those of IABP and IAPCGP, contains an amide bond. We propose that the presence of potential

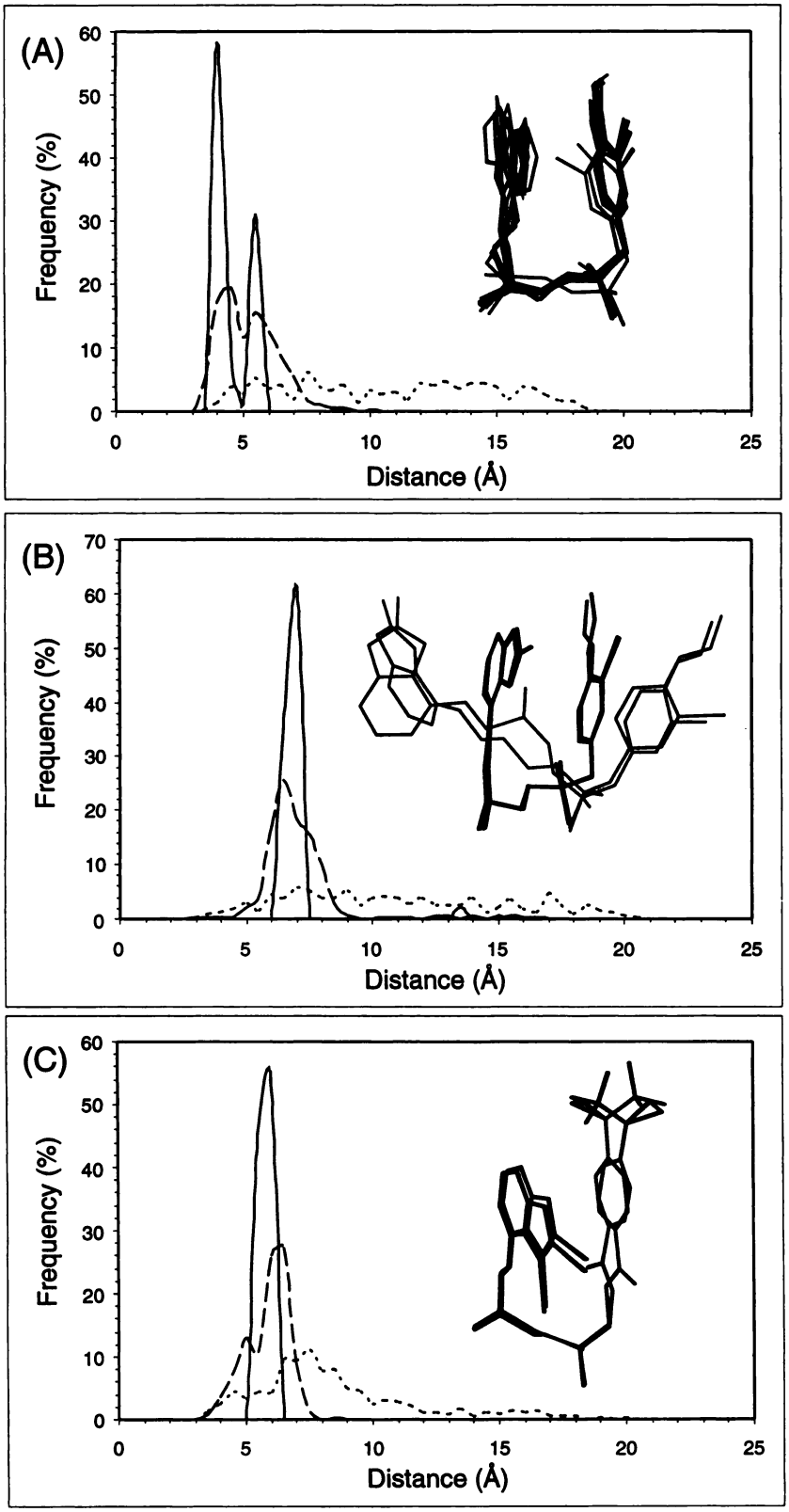


**Fig. 7.** Inter-ring distances from molecular dynamics simulation of IABP, IAPCGP, and ICYPdz. The distances between the photoreactive group and the 1-nitrogen on the opposite ring of IABP (A), IAPCGP (B), and ICYPdz (C) are plotted for the initial high temperature simulation (*dotted line*), the conformers re-equilibrated at 300° K (*dashed line*), and the final energy-minimized conformation for each (*solid line*). *Insets*, bundles of the final lowest energy conformations.

hydrogen bond participants in the alkylamine region of ICYPdz may lead to interactions with the receptor that stabilize a conformation that favors derivatization of TM 1.

Supporting evidence for this scenario can be found in a previous study that used the affinity label pBABC (27). pBABC is structurally similar to ICYPdz and also contains an amide bond in the alkylamine region. Dohlman *et al.* (9) reported derivatization of a site within amino acids 83-96 (TM 2) of the hamster lung $\beta_2$AR and evidence for a minor site of derivatization in TM 4. It is interesting to note that both ICYPdz and pBABC seem to greatly favor derivatization of adjacent sites (TM 1 and TM 2, respectively) within the

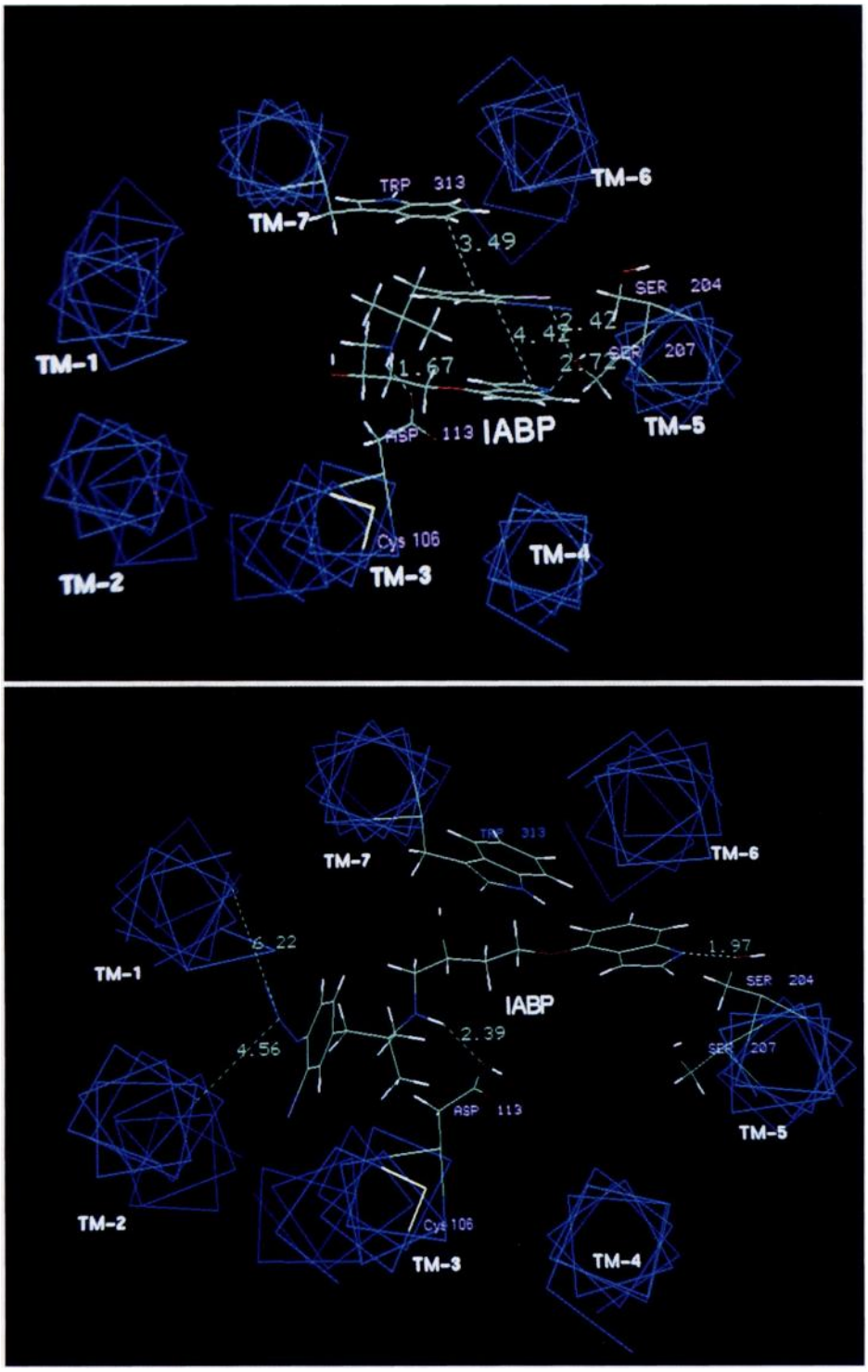


**Fig. 8.** Illustrative model for the interaction of two IABP conformers with the $\beta_2$AR. The transmembrane region of the $\beta_2$AR was modeled using the Insight II package (Biosym Technologies, San Diego, CA). The seven TM segments were built as $\alpha$ helices. The helices were initially aligned with the structure of bacteriorhodopsin and were rotated about their helical axes to bring the known functional groups ($Asp^{113}$, $Ser^{204}$, $Ser^{207}$) into the core of the molecule. Representative folded and extended conformations of IABP were chosen from the molecular dynamics simulations. These were positioned in the model so that the alkylamine was within bonding distance $Asp^{113}$ and the indole amine was within hydrogen bonding of $Ser^{204}$ and $Ser^{207}$. $Trp^{313}$, a probable site of derivatization (8), was also included. *Numbers in green*, distances (in Å). *Top*, hypothetical interactions allowing labeling of $Ser^{207}$ by IABP. *Bottom*, hypothetical interactions allowing labeling of TM 1 by IABP. A hydrogen bond between the indole amine and $Ser^{204}$ is shown, but a hydrogen bond between the the aryloxy oxygen and $Asn^{312}$ (not shown), as proposed by Suryanarayana *et al.* (26), is also possible.

ligand binding site. Dohlman *et al.* concluded that the site of derivatization by pBABC in TM 2 is most likely $His^{93}$. If so, $Ser^{92}$ could form a hydrogen bond with the amide of pBABC, which is directly adjacent to the reactive bromoacetyl group. The derivatization of TM 1 by ICYPdz is consistent with such an interaction as the photoactive diazarene moiety is several Angstroms removed from the amide (see Fig. 1).

The unique properties of salmeterol are one indication that the alkylamine moieties of βAR ligands can have pharmacological significance. The extremely long duration of action of this $\beta_2$AR agonist is dependent on the presence of an ether oxygen in the alkylamine group (28). It is tempting to speculate that the interactions that favor derivatization of TM 1 by ICYPdz and of TM 2 by pBABC are analogous to those that contribute to the unique properties of salmeterol.

The differences in the labeling patterns of IABP and IAPCGP are more difficult to interpret. These two compounds differ only slightly in the aryloxy end (indoloxy versus benzimidazolonoxy) and are otherwise identical (see Fig. 1). Therefore, the differences in labeling patterns cannot be

dictated based on differences in the alkylamino end of these photoaffinity labels. Both of these compounds derivatized TM 5, but only IAPCGP derivatized TMs 2 and 3 and (along with ICYPdz) TM 4. One interpretation of the derivatization of TM 5 by both compounds is that the aryloxy ends of IABP and IAPCGP interact to some extent with TM 5, and folded conformations of these molecules enable them to label TM 5, just as we proposed for TMs 6 and 7.

The selectivity of IABP for $Ser^{207}$ in TM 5 over other sites in the 30-kDa tryptic peptide may be due to a conformation-stabilizing hydrogen bond between $Ser^{204}$ and the indole amine of IABP. The similarity between the inter-ring distance predicted for IABP (4.0-5.5 Å, Fig. 7A) and the rise of three residues ($Ser^{204-207}$) along an $\alpha$ helix (4.5 Å) supports this possibility. A model for this interaction is shown in Fig. 8. Such an interaction has been proposed as a mechanism for the partial agonist properties of pindolol in some tissues and mutant receptors (29). A similar interaction between TM 5 and IAPCGP via a benzimidazole-2-one nitrogen could account for IAPCGP derivatization of TM 5. Likewise, derivatization of TM 4 by IAPCGP and ICYPdz could reflect interactions between the aryloxy ends of these molecules with TM 4. The observation that both IAPCGP and ICYPdz include polar substituents (carbonyl and cyano, respectively) at the 2 position on the heterocyclic aryloxy ring suggests a molecular basis for TM 4 labeling by IAPCGP and ICYPdz but not IABP. The discovery that some $\beta$AR antagonists are also inverse agonists (30) suggests a possible pharmacological role for different interactions with the receptor by structurally similar compounds.

IAPCGP also derivatizes TMs 2 and 3 to a small extent. Because IABP, which is identical to IAPCGP in the alkylamino end, does not derivatize TMs 2 and 3, it seems likely that some intrinsic property of the benzimidazole-2-one moiety of IAPCGP is responsible for this difference. Because the 6-kDa peptide for TMs 2 and 3 contains the counter ion for the ligand amino nitrogen ($Asp^{113}$), labeling of this peptide implies that IAPCGP can assume a conformation that holds the aryl azide moiety in close proximity to the amino nitrogen and away from the aryloxy end. Molecular dynamics analysis of IAPCGP predicts a small population of IAPCGP conformers with an inter-ring distance of 12-13 Å, which is not predicted for IABP (Fig. 7, A and B). Thus, these conformations meet the two criteria for agreement with IAPCGP labeling of TMs 2 and 3: they are unique to IAPCGP, and they bring the photoactive group away from the aryloxy end of the molecule and close to the amino nitrogen.

We have shown, using the unique photoaffinity label IAPTA, that the aryloxy end of the $\beta$-antagonist pharmacophore is highly constrained within the vicinity of TMs 6 and 7. With the $\beta$-antagonist photoaffinity labels IABP, IAPCGP, and ICYPdz, we showed that the amino end of the $\beta$-antagonist pharmacophore is able to assume several conformations within the ligand binding site. Heterogeneity in the location and intensity of derivatization were dictated by minor structural differences in both the alkylamino and aryloxy moieties of the photolabels studied. Experiments with site-directed mutagenesis of the $\beta_2$AR could further resolve which amino acids permit the distinctive labeling patterns observed with these photoaffinity labels in the wild-type receptor.

**Acknowledgments**

We thank Dr. Marty Arbabian and Dr. Vahid Hekmat for expert technical assistance and Dr. William A. Catterall for critical review of the manuscript.

**References**

1. Frielle, T., S. Collins, K. W. Daniel, M. G. Caron, R. J. Lefkowitz, and B. K. Kobilka. Cloning of the cDNA for the human $\beta_1$-adrenergic receptor. *Proc. Natl. Acad. Sci. USA* **84:**7920-7924 (1987).
2. Dixon, R. A. F., B. K. Kobilka, D. J. Strader, J. L. Benovic, H. G. Dohlman, T. Frielle, M. A. Bolanowski, C. D. Bennett, E. Rands, R. E. Diehl, R. A. Mumford, E. E. Slater, I. S. Sigal, M. G. Caron, R. J. Lefkowitz, and C. D. Strader. Cloning of the gene and cDNA for mammalian $\beta$-adrenergic receptor and homology with rhodopsin. *Nature (Lond.)* **321:**75-79 (1986).
3. Emorine, L. J., S. Marullo, M. M. Briend-Sutren, G. Patey, K. Tate, C. Delavier-Klutchko, and A. D. Strosberg. Molecular characterization of the human $\beta_3$-adrenergic receptor. *Science (Washington D. C.)* **245:**1118-1121 (1989).
4. O'Dowd, B. F., R. J. Lefkowitz, and M. G. Caron. Structure of the adrenergic and related receptors. *Annu. Rev. Neurosci.* **12:**67-83 (1989).
5. Tota, M. R., M. R. Candelore, R. A. F. Dixon, and C. D. Strader. Biophysical and genetic analysis of the ligand binding site of the $\beta$-adrenoceptor. *Trends Pharm. Sci.* **12:**4-6 (1990).
6. Dixon, R. A. F., I. S. Sigal, E. Rands, R. B. Register, M. R. Candelore, A. D. Blake, and C. D. Strader. Ligand binding to the $\beta$-adrenergic receptor involves its rhodopsin-like core. *Nature (Lond.)* **326:**73-77 (1987).
7. Tota, M. R., and C. D. Strader. Characterization of the ligand binding domain of the $\beta$-adrenergic receptor with the fluorescent antagonist carazolol. *J. Biol. Chem.* **265:**16891-16897 (1991).
8. Wong, S. K., C. Slaughter, A. E. Ruoho, and E. M. Ross. The catecholamine binding domain of the $\beta$-adrenergic receptor is formed by juxtaposed membrane-spanning domains. *J. Biol. Chem.* **263:**7925-7928 (1988).
9. Dohlman, H. G., M. G. Caron, C. D. Strader, N. Amlaiky, and R. J. Lefkowitz. Identification and sequence of a binding site peptide of the $\beta_2$-adrenergic receptor. *Biochemistry* **27:**1813-1817 (1988).
10. Strader, C. D., I. S. Sigal, M. R. Candelore, E. Rands, W. S. Hill, and R. A. F. Dixon. Conserved aspartic acid residues 79 and 113 of the $\beta$-adrenergic receptor have different roles in receptor function. *J. Biol. Chem.* **263:** 10267-10271 (1988).
11. Strader, C. D., M. R. Candelore, W. S. Hill, I. S. Sigal, and R. A. F. Dixon. Identification of two serine residues involved in agonist activation of the $\beta$-adrenergic receptor. *J. Biol. Chem.* **264:**13572-13575 (1989).
12. Hassan, M., and M. Goodman. Computer simulations of the conformations of catecholamine derivatives. *Ann. N. Y. Acad. Sci.* **446:**185-198 (1985).
13. Blin, N., L. Camoin, B. Maigret, and A. D. Strosberg. Structural and conformational features determining selective signal transduction in the $\beta_3$-adrenergic receptor. *Mol. Pharmacol.* **44:**1094-1104 (1993).
14. Rashidbaigi, A., and A. E. Ruoho. Iodoazidobenzylpindolol, a photoaffinity label for the $\beta$-adrenergic receptor. *Proc. Natl. Acad. Sci. USA* **78:**1609-1613 (1981).
15. Ruoho, A. E., A. Rashidbaigi, G. H. Hockerman, M. Larson, J. F. Resek, and C. C. Malbon. Development of novel photoaffinity ligands for the $\beta$-adrenergic receptor. *Neuroprotocols* **4:**50-65 (1994).
16. Caron, M. G., Y. Srinivasan, J. Pitha, K. Kociolek, and R. J. Lefkowitz. Affinity chromatography of the $\beta$-adrenergic receptor. *J. Biol. Chem.* **254:** 2923-2927 (1979).
17. George, S. T., M. A. Arbabian, A. E. Ruoho, J. Kiely, and C. C. Malbon. High efficiency expression of mammalian $\beta$-adrenergic receptors in baculovirus-infected insect cells. *Biochem. Biophys. Res. Commun.* **163:**1265-1269 (1989).
18. Fling, S. P., and D. S. Gregerson. Peptide and protein molecular weight determination by electrophoresis using a high-molarity Tris buffer system without urea. *Anal. Biochem.* **155:**83-88 (1986).
19. Hunkapiller, M. W., E. Lujan, F. Ostrander, and L. E. Hood. Isolation of microgram quantities of proteins from polyacrylamide gels for amino acid sequence analysis. *Methods Enzymol.* **91:**227-236 (1983).
20. G. L. Peterson. A simplification of the protein assay method of Lowry et al. which is more generally applicable. *Anal. Biochem.* **83:**346-356 (1977).
21. Schaffner, W., and C. Weismann. A rapid, sensitive, and specific method for the determination of protein in dilute solutions. *Anal. Biochem.* **56:**502-514 (1973).
22. Dohlman, H. G., M. Bouvier, J. L. Benovic, M. G. Caron, and R. J. Lefkowitz. The multiple membrane spanning topography of the $\beta_2$-adrenergic receptor. *J. Biol. Chem.* **262:**14282-14288 (1987).
23. Houmard, J., and G. R. Drapeau. Staphylococcal protease: a proteolytic enzyme specific for glutamoyl bonds. *Proc. Natl. Acad. Sci. USA* **69:**3506-3509 (1972).
24. Henderson, R., J. M. Baldwin, T. A. Ceska, F. Zemlin, E. Beckman, and K. Downing. Model for the structure of bacteriorhodopsin based on high resolution electron cryomicroscopy. *J. Mol. Biol.* **213:**899-929 (1990).
25. Kobilka, B. K., T. S. Kobilka, K. Daniel, J. W. Regan, M. G. Caron, and R. J. Lefkowitz. Chimeric $\alpha_2$-, $\beta_2$-adrenergic receptors: delineation of domains

involved in effector coupling and ligand binding. *Science (Washington D. C.)* **240**:1310-1316 (1988).
26. Suryanarayana, S., and B. K. Kobilka. Amino acid substitutions at the position 312 in the seventh hydrophobic segment of the $\beta_2$-adrenergic receptor modify ligand binding specificity. *Mol. Pharmacol.* **44**:111-114 (1993).
27. Dickinson, K. E. J., S. L. Heald, P. W. Jeffs, R. J. Lefkowitz, and M. G. Caron. Covalent labeling of the β-adrenergic ligand-binding site with para-(bromoacetamidyl)benzylcarazolol, a highly potent β-adrenergic affinity label. *Mol. Pharmacol.* **27**:499-506 (1985).
28. Nials, A. T., M. J. Sumner, M. Johnson, and R. A. Coleman. Investigations into factors determining the duration of action of the $\beta_2$-adrenoceptor agonist, salmeterol. *Br. J. Pharmacol.* **108**:507-515 (1993).
29. Strader, C. D., M. R. Candelore, S. W. Hill, R. A. F. Dixon, and I. A. Sigal. A single amino acid substitution in the β-adrenergic receptor promotes partial agonist activity from antagonists. *J. Biol. Chem.* **264**:16470-16477 (1989).
30. Bond, R. A., P. Leff, T. D. Johnson, C. A. Milano, H. A. Rockman, T. R. McMinn, S. Apparsundaram, M. F. Hyek, T. P. Kenakin, L. F. Allen, and L. J. Lefkowitz. Physiological effects of inverse agonists in transgenic mice with myocardial overexpression of the $\beta_2$-adrenoceptor. *Nature (Lond.)* **374**:272-276 (1995).

**Send reprint requests to:** Dr. Arnold E. Ruoho, Department of Pharmacology, University of Wisconsin School of Medicine, 1300 University Avenue, Madison, WI 53706. E-mail: aeruoho@facstaff.wisc.edu